Photochemistry of nabumetone in aqueous solution of sodium dodecylsulfate (SDS) micelles

Margarita Valero*[,a], Peter P. Levin[b,c], Natalya B. Sultimova[b] , Judith E. Houston[d,e]

[a] Dpto. Química Física, Facultad de Farmacia, Universidad de Salamanca, Campus Miguel de Unamuno, s/n, 37007 Salamanca, Spain

[b] Emanuel Institute of Biochemical Physics, Russian Academy of Sciences, Moscow, Russia, 119334

[c] Semenov Institute of Chemical Physics, Russian Academy of Sciences, Moscow, Russia, 119334

[d] Jülich Centre for Neutron Science (JCNS) at Heinz Maier-Leibnitz Zentrum (MLZ) Forschungszentrum Jülich GmbH, Lichtenbergstraße 1, 85747 Garching, Germany.

[e] European Spallation Source (ESS), Odarslövsvägen 113, 225 92 Lund, Sweden.

*Corresponding author: mvalero@usal.es

Abstract

The photochemistry, solubility and distribution between two phases of nabumetone (NB) in aqueous solution of sodium dodecylsulfate (SDS) micelles were studied. The solubility (S_{NB}) of NB was monitored using steady-state UV-Vis absorption spectroscopy. The linear relationship of S_{NB} to SDS concentration ([SDS]) gave the large value of partition coefficient, P (logP = 3.5), for NB distribution between the aggregate and the water phase showing the localization of NB in the micellar phase. NB fluorescence (FL) quantum yield increases with [SDS] from 0.03 in water to 0.056 at 0.2M [SDS]. The dependence of FL intensity at 355 nm (F_{335}) on [SDS] is bell-shaped. The plot of initial F_{335} increase with [SDS] in the range 0 - 0.05 M gave the expected value of the critical micelle concentration (cmc = 7.9 mM). Further increase of [SDS] resulted in 10% decrease of F_{335} demonstrating the variation of the micellar structure. Small-Angle Neutron Scattering (SANS) and refractometry confirmed this variation. The NB in SDS was protected against photodegradation. High Performance Liquid Chromatography/Mass Spectrometry (HPLC/MS) detected 2-(but-2-en-1-yl)-6-methoxynaphthalene as NB final photoproducts in SDS solution which was not found in homogeneous media. The hydrated electron localized in water phase, NB radical cation and

ABBREVIATIONS

NB: Nabumetone

NSAID: non-steroidal anti-inflammatory drug

SDS: sodium dodecylsulfate

SANS: small angle neutron scattering

NB triplet excited state both localized in the micellar phase were observed by laser flash photolysis of NB in micellar solution. The decay kinetics of these intermediates was different with respect to that in the homogeneous media. The reactivity of NB in SDS micellar environment compared to the homogeneous media is under the discussion.

Key words

Nabumetone, sodium dodecyl sulfate (SDS), small angle neutron scattering (SANS), photochemistry, fluorescence, laser flash photolysis.

1. Introduction

Nabumetone (NB, Scheme 1), is one of the most prescribed non-steroidal anti-inflammatory drugs (NSAID), which is widely used to treat osteoarthritis in humans [1] as well as in veterinary [2]. NB is a prodrug which is almost completely metabolized in the liver to the active metabolite, 6-methoxy-naphthyl-acetic acid. In comparison with other NSAIDs NB presents a comparable efficacy but lower side effects [1].

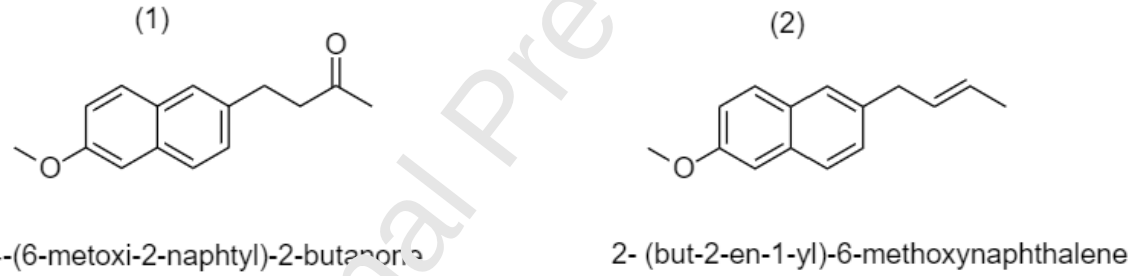

Scheme 1: Chemical structure of nabumetone **(1)** (*left*) and the photoproduct found after drug irradiation in aqueous SDS solution **(2)** (*right*).

NSAIDs are well known photosensitizing agents [3]. This is the reason for side effects which are observed for 0.1 – 1% of patients treated with NB (as specified in the directions for use included in the commercial formulations of the drug, for instance, in relifex® and relief®). However, scarce research on NB photochemistry [4] and phototoxicity [5] has been performed in contrast with other NSAIDs.

Although, nowadays, a new scenario has emerged namely the occurrence of pharmaceuticals in fresh waters all over the world [6]. Specifically, NB, coming from sewage, has been recently detected in Jiaozhou Bay, in China [7]. It is important to note, that hydrophilic pharmaceuticals persist in water, whereas hydrophobic ones accumulates in hydrophobic pools, as demonstrated for organic matter [8]. On these basis it can be expected pharmaceuticals accumulate in biological hydrophobic domains, such as skin or membranes.

So, it is of paramount importance, from pharmaceutical and ecological point of view, to study the photochemical behavior of the drug itself, not only in water, but also in complex biological structures. Up to date, the photochemical behavior of NB in water [9] and other homogeneous media was reported [10], but similar results for more complex systems are scarce [5].

Micelles, are interesting systems as biomimetic models and well known supercages where the reactivity of the loaded compounds becomes different with respect to that in homogeneous media. In this regard, studies of photodegradation of chemicals have been carried out in several micellar solutions [11–14]. The results have demonstrated that micellar environment can either increase [11,13,14] or decrease [11,12,14] the photodegradation of chemicals, including pharmaceuticals, and natural products.

The detergent sodium dodecyl sulfate (SDS) is usually present in water coming from personal care products [13]. And it is currently used as excipient in some commercialized formulation of the NB (relafén®). It has been frequently used as biomimetic model in the study of the photochemical behavior of different drugs [11,15–17].Therefore, we found that SDS is a good choice as biomimetic model for the study of NB photochemical behavior.

Thus, in the present work the solubility, photochemical behavior of NB in SDS micelles as well as the characteristics of free and NB loaded aggregates were studied using different techniques. The photodegradation, nature and kinetics of reaction intermediates and final photoproducts were examined.

The investigation was performed in order to get information about NB photochemistry in organized biological like structures, for toxicological and cleaning purposes.

The results show that NB is localized in SDS micelles, where it adopts a folded conformation. SDS protects NB against photodegradation in contrast to other hydrophobic medium [10]. A final photoproduct with reduced lateral side chain was found after drug irradiation in SDS micelle. Flash photolysis of NB in SDS shows the formation of three transients, namely triplet state, ^{3}NB, radical cation, $NB^{+\bullet}$, and hydrated electron, e_{aq}^{SDS}. The reactions of ^{3}NB and e_{aq}^{SDS} with molecular oxygen are controlled by diffusion and it is expected to result in the formation of active forms of oxygen. In contrast to the homogeneous solutions the decay of $NB^{+\bullet}$ in SDS micelle was found to be second order and proceeded by backward electron transfer from species located in the aqueous phase with regeneration of starting NB.

2. Experimental section

2.1. Materials

Nabumetone, (NB, 6142), analytical standard, was obtained from Sigma. Sodium dodecyl sulfate, (SDS, 230425000) for biochemistry, 99% purity, was purchased from Agros Organic. The chemicals were used as received.

D_2O (Sigma Aldrich, 99.8% purity) was used instead of water for the preparation of the samples for small-angle neutron scattering (SANS) measurements. For all other experiments, samples were prepared with ultrapure water (18.2 MΩ·cm, Millipore-filtered).

2.2. Solutions

Aqueous stock solutions of (1) SDS, 0.2 M, (2) NB, 0.04 mM and (3) NB, 1 mM with SDS, 0.2 M, were initially prepared under mechanical stirring. The solutions with different concentrations of NB and SDS were obtained by mixing appropriate amounts of the stock solutions.

For solubility determination, fixed volume of the aqueous solutions with different SDS concentration, in the range of 0.02-0.2 M, prepared by diluting solution (1) was added to an excess of solid NB weighted in a topaz vial.

For SANS, a stock solution of SDS 0.2M in D_2O was prepared. 1 mM NB in 0.05 or 0.2 M SDS solutions in D_2O were prepared by drug weighing and solubilizing.

Irradiated 1mM NB in 0.2M SDS aqueous solution was analyzed by High Performance Liquid Chromatography /Mass spectrometry (HPLC/MS).

In laser flash photolysis experiments SDS and NB concentrations were 0.2 M and 0.5 - 3 mM, respectively.

2.3. Methods

2.3.1. Uv-vis absorption and Emission spectroscopies

In the solubility determination, solutions were mechanically stirred during 72h in a dark room thermostated at 20 ºC. Saturated solutions were centrifuged in a P-Selecta centrolit, with a max 12000 rpm, during 10 min. The supernatant was then diluted with water or SDS of the appropriate concentration, and NB concentration was determined by UV-Vis absorption spectroscopy.

Measurements were performed on UV-Vis Hitachi, model 150-20, spectrophotometer. Absorption spectrum was obtained in the range λ = 250-450 nm, in a quartz cuvette with 1cm pathlength, using Milli Q water as a reference. NB absorption spectrum shows characteristic bands centered at 317 and 330 nm [9][10][18]. The NB concentration was determined from the value of optical density at 330 nm, using corresponding extinction coefficients $\varepsilon_{330}^{NB:H2O}$=780 $M^{-1}cm^{-1}$ (previously reported, ε_{330}^{H2O}=730 M^{-1} cm^{-1} [10]) and $\varepsilon_{330}^{NB:SDS}$=1000 M^{-1} cm^{-1}, and corrected with SDS contribution using $\varepsilon_{330}^{SDS:H2O}$ = 0.34 M^{-1} cm^{-1}, all of them were experimentally determined in this work.

Steady-state fluorescence emission and excitation spectra were recorded with a Perkin Elmer LS 50B spectrofluorimeter with the thermostated sample holder. The spectra were corrected using software provided with the apparatus.

The emission spectra in wavelength range λ_{em}= 325-450 nm were obtained with λ_{exc}= 317 nm. The excitation spectra were measured at λ_{em}= 355 and 440 nm.

SDS cmc values were obtained by fitting the plots of fluorescence or refractive index data (P) vs. [SDS] to a logistic equation as described in [19,20].

The fluorescence quantum yields, ϕ_f, were measured using the reference quantum yield (0.543) for quinine sulfate in 0.1N sulfuric acid [21]).

Refractive index was measured in a Shibuya Optical refractometer.

2.3.2. Small-Angle Neutron Scattering (SANS)

SANS experiments were carried out on the KWS-2 diffractometer at the Jülich Centre for Neutron Science (JCNS), Münich, Germany [22]. An incidental wavelength of 5 Å was used with detector distances of 1.7 and 7.6 m and a collimation length of 8 m, to cover a momentum transfer, q, range from 0.008 to 0.5 $Å^{-1}$. In the standard mode, a wavelength spread $\Delta\lambda/\lambda$= 20% was used. All samples were measured in quartz cells (Hellma) with a path length of 2 mm using D_2O as the solvent. The samples were placed in an aluminum rack where water was recirculated from an external Julabo cryostat, at 25 ºC. This set-up enables a thermal control with up to 0.1 ºC precision. Scattered intensities were corrected for detector pixel efficiency, empty cell scattering and background due to electronic noise. The data were set to absolute scale using Plexiglas as a secondary standard. The obtained macroscopic differential cross-section $d\Sigma/d\Omega$ was further corrected for the contribution from the solvent. The complete data reduction process was performed with the QtiKWS software provided by JCNS in Garching [22].

Solutions of SDS with two concentrations (0.05 and 0.2 M) without and with 1 mM of NB were studied. All samples were measured in D_2O in order to optimize the contrast and minimize the incoherent background in SANS experiments.

SANS curves were fitted using SAS View 4.2.1. software to an ellipsoid model (S1) [23,24] with a Hayter-Penfold MSA interparticle structure factor S(Q) for charged particles. The parameter $sld_{SDS\ micelle}$ -0.237 × 10^{-6} $Å^{-2}$, a dielectric constant of D_2O =77.936 [25] and the scale factor equal to 1 were fixed.

The aggregation number was determined as described in [26].

2.3.3. Photodegradation

Heraeus Noblelight photoreactor, with UV immersion lamp TQ 150 (high pressure mercury lamp), with emission maxima at λ = 365 nm and 313 nm (with lower intensity), was used to irradiate the solutions.

The wavelength of the radiation implicated in the most of the phototoxic processes was in the range from 300 to 400 nm [27].

The incident light intensity (I_0) was detected by a potassium ferroxilate actinometer solution (0.006 M) at 365 nm, with Φ=1.21 [28], assuming total light absorption by the actinometer

[29] and. using the method described elsewhere [27]. The intensity of the irradiating lamp was 4.15×10^{-6} Einstein L^{-1} s^{-1}.

The phototodegradation quantum yield of NB, ϕ_{PD}, was calculated from the experimental photodegradation rate constant, $k_{PD,}$ as described in [30], using the characteristics of the photoreactor provided by the manufacturer.

2.3.4. High Performance Liquid Chromatography /Mass spectrometry (HPLC/MS)

High Performance Liquid Chromatography-mass spectrometry (HPLC/MS) analysis was made with an Waters ZQ4000 equipment, with HPLC Waters Alliance 2795.

The conditions used in HPLC were: Xbridge C18 column (100 mm length x 2.1 mm diameter and with 3.5 μm of particle size). Binary mixtures of Solvent A: water with 0,1% formic acid and Solvent B: acetonitrile, with gradient included in S2 were used. The flux was 0,2 mL/min.

Detection using diode array from 200-600 nm and quadrupole mass spectrometry with ionization by electrospray in positive way.

2.3.5. Flash Photolysis

The absorption spectra and the decay kinetics of intermediates were measured using the nanosecond laser photolysis apparatus with the registration of UV-Vis absorption at a given wavelength in the range 400 – 800 nm [31,32].

Nitrogen laser (PRA LN 1000, with 1 ns pulse duration and 337 nm radiation wavelength, operating in the 10 Hz frequency mode) was used as an excitation source. Acquisition and averaging of kinetic curves were performed by a UF258 transient recorder for PCI bus, connected with a personal computer. Each experimental kinetic curve contained 12–14 bits of points, with the distance between points being 2–400 ns. Dissolved air oxygen was removed by Ar bubbling during 20 min. All measurements were carried out in a quartz cell with an optical path length of 2 mm at 25 °C.

3. Results and Discussion

3.1. Nabumetone in aqueous SDS solution.

3.1.1. Nabumetone Solubility in Aqueous SDS Solutions.

The solubility, S_{NB}, of NB in water , $S_{NB}^{H_2O}$, and in aqueous SDS solutions, S_{NB}^{SDS}, at different surfactant concentrations, in a range 20-200 mM (all above cmc=8.14 [33], 8.2 mM [34]) was determined using UV-Vis absorption spectroscopy. The S_{NB}^{SDS}, (S3), increases significantly with [SDS] up to 0.033 M at 0.2 M of SDS (5.4% wt/v), which is nearly 80 times larger than in water

The plot of $S_{NB}^{SDS}/S_{NB}^{H_2O}$ vs. surfactant volume fraction, ϕ_{SDS}, (calculated using SDS molar volume $\bar{V}_{SDS}$ =0.288 L/M) [35]) is linear (Figure 1).

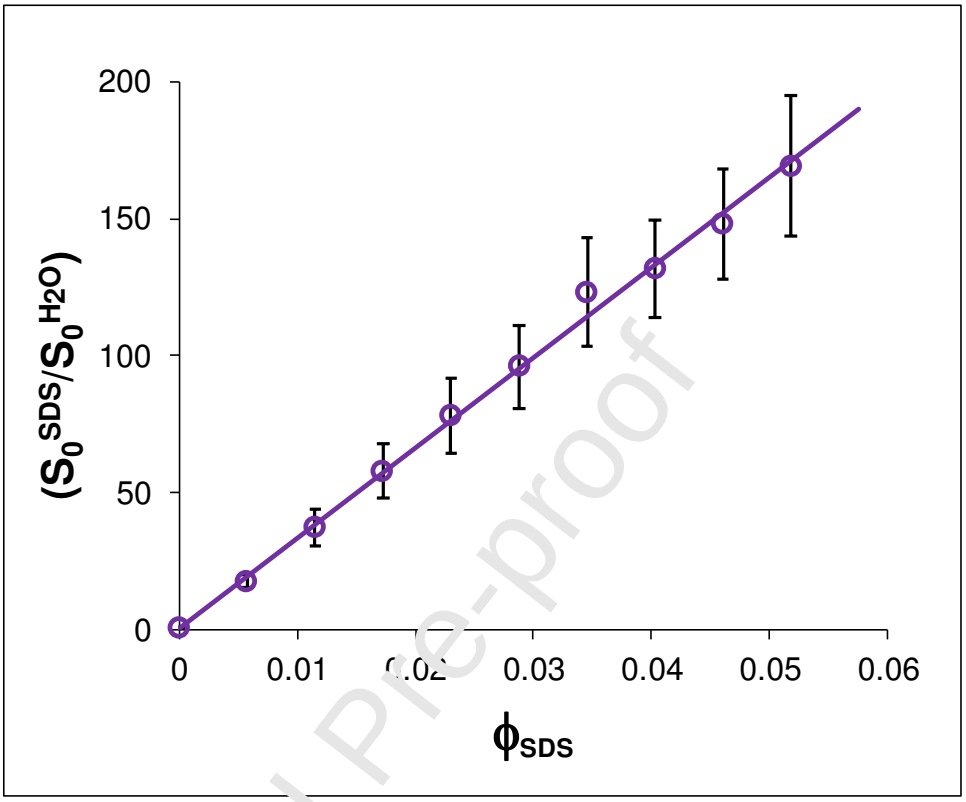

Figure 1: Plot of the ratio of NB solubility in SDS and in water ($S_0^{SDS}/S_0^{H_2O}$) vs. SDS volume fraction (ϕ_{SDS}). The line is the fitting to the linear function.

According to Collet et al. [36], the slope of this linear dependence corresponds to the partition coefficient, P, of NB between micellar and water phases, which is equal to 3278 ± 72, logP=3.5. This value is large enough to demonstrate that NB is localized in micellar phase. Therefore, one can suppose that NB accumulates in the nonpolar biological structures such as skin or membranes and in the cells by this way. Gastro-intestinal, GI, alterations are common NB side effects. The mechanism of these side effects is not well known, however it has been found that NSAIDs are accumulated in gastric cells at acidic pH [37]. The high local concentration of NB could be responsible for the GI side effects.

It is worthwhile mentioning that we obtained the value of the solubility of NB in water (S3) $S_{NB}^{H_2O}$= 0.41 mM ($9.3*10^{-2}$ mg/mL), which is significantly larger than those previously reported ($2.4*10^{-3}$ mg/mL [38] or $1.9*10^{-2}$mg/mL [39]). In all those studies, saturated samples were filtered, while in the present work they were centrifuged, which could justify the difference.

3.1.2. Steady-state Fluorescence of Nabumetone in Aqueous SDS Solutions.

Steady-state fluorescence spectra, of NB at two drug concentrations, 0.04 and 1 mM. in the presence of increasing amounts of SDS were obtained (S4). NB fluorescence in water is characterized by the band with maximum at λ_{em}=355 nm, as previously reported [5][40]. At low NB concentration, 0.04 mM, the increase of [SDS] up to 10 mM results in more than two times increase of fluorescence intensity at 355 nm, F_{355}, followed by a plateau (Figure 2A).

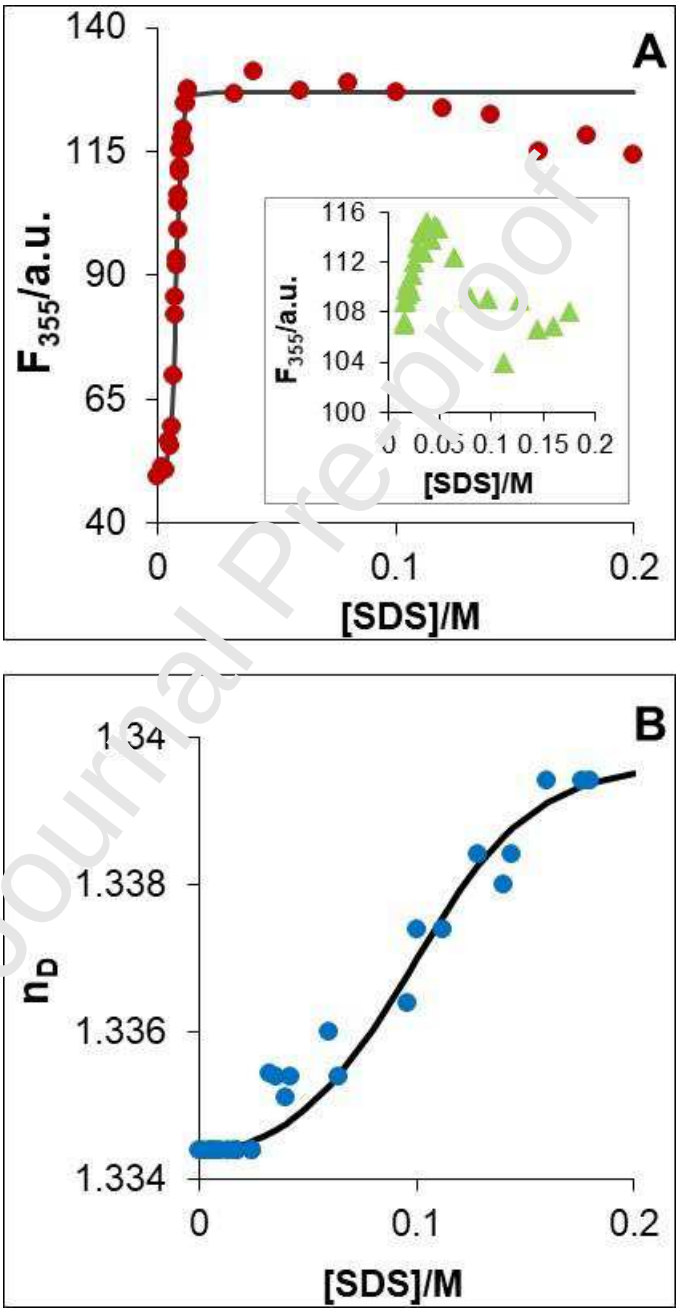

Figure 2. A: The plot of fluorescence intensity at 355 nm, F_{355}, of NB, 4×10^{-5}M (●) and: 1 mM (▲) (*Inset)* and **B** - Refractive index of all the samples, 0.04 and 1mM of NB vs. SDS concentration (●). Black solid line in A and B is the fitting to a logistic equation [19,20].

In this concentration range, the variation of NB fluorescence intensity with SDS concentration fits successfully to a logistic equation [19,20]. An inflection point, appears at 7.9 mM, which corresponds to the cmc of spherical (ellipsoid) SDS micelles formation, as previously reported, cmc=8.14 [33] or 8.2 mM [34]. Therefore, the observed increase of fluorescence intensity is due to SDS micelle formation followed by localization of NB in micellar phase. The saturation of the fluorescence intensity at large SDS content clearly shows that the most part of NB localizes in micellar phase.

However, the increase of SDS concentration above 0.1 M leads to a quenching of NB fluorescence, indicating some change in NB due to the restructuration of micelles (Figure 2A). The same trend is observed at large, 1 mM, NB concentration (Figure 2A inset). The quenching of NB FL intensity starts above [SDS]= 50 mM. Similarly, a decrease in the UV-Vis absorptivity of morin was observed above [SDS]= 60 mM, and this value was assumed as the cmc of SDS rod micelles formation [41].

The variation of micellar structure with micellar growing results in the increase in the refractive index [42]. The plot of refractive index vs. [SDS] is of sigmoid form for both [SDS] (Figure 2B). The data adequately fit to a logistic equation [19,20] with the inflection point at 98 mM. This cmc value for the rod SDS micelles formation is similar to that extracted with morin as a probe [41].

The FL quantum yield of NB determined for diluted NB solutions at the highest 0.2 M [SDS], ϕ_{FL}=0.056, is higher than those in water ϕ_{FL}=0.03 and in β-CD, ϕ_{FL}=0.045, but significantly smaller than that in α-CD, ϕ_{FL}=0.467 [43]. The inclusion complex of NB with α-CD occurs through the lateral side chain avoiding its interaction with the naphthalene moiety, resulting in the high quantum yield of the drug [40]. By contrast, NB was assumed to be half folded or folded, with different lateral side chain and naphthalene ring mutual orientation and interaction in β-CD inclusion complex or free in water, which results in lower fluorescence quantum yield as this interaction is stronger [43]. Then, the fluorescence quantum yield value, points to a closed conformation of NB in the SDS micelle. Moreover, the intra-molecular interaction between the lateral side chain and naphthalene ring seems to be stronger at high surfactant concentration. Interestingly, the NB folded conformation is preferred for binding to the cytochrome enzyme CYP1A2, the hepatic enzyme involved in its metabolism [44]. The active site of the enzyme, is compact, narrow and able to bind flat aromatic molecules, features that are likely reproduced in the micelle.

3.1.3. Small-Angle Neutron Scattering, SANS, Study of SDS Aggregates

In order to get some information about the changes in the micelle with SDS concentration, free and NB-loaded SDS aggregates, formed at surfactant concentrations of 50 and 200 mM, were studied by SANS.

SANS curves (Figure 3), show a correlation peak characteristic of interacting charged micelles in solution [45], with an upturn in the scattering curve at low q, related to the existence of interactions between the micelles, which was previously described for SDS [46]. This upturn was considered to originate from attractive, entropy-driven depletion interactions that appear in mixtures of rod and spheres [47,48].

As it can be observed in Figure 3A, SANS curves for NB-loaded SDS are quite similar to those for the free micelle, except at low q. The presence of NB decreases the attractive depletion interactions, up to the complete disappearance at high SDS concentration; this effect was also observed in the presence of added salts [46]. The q scaling of upturn slope at low q (around 4), suggests the presence of larger fractals [49] of SDS micelles, which are consequently broken by the addition of NB. The decrease in the attractive interactions among the aggregates could be at the origin of this effect.

The increase in SDS concentration produces a strong increase in the scattering intensity and shift of the peak towards higher q values. The peak position is related to the average distance between micelles, d, as $q_{max} \sim 2\pi/d$. The value of d decreases from 113 to 81 Å with [SDS] increase from 0.05 to 0.2 M. The latter is in good agreement with d=86 Å published for 0.3 M of SDS [50].

The curves were fitted to different models: sphere, cylinder (S5 and S6) and ellipsoid (Figure 3, Table 1) for all the systems. The best fitting of the SANS curves, in most of the systems, is to an ellipsoidal model of micelle (Figure 3B) (Table 1), as previously described [51]. However, the SANS curves measured at high SDS concentration in the presence of NB, fits even slightly better to a cylindrical model (S6, S7) rather than to the ellipsoid one. The change in the micelle shape with surfactant concentration predicted by fluorescence and refractive index is not confirmed by SANS. However, SANS reveals some additional features due to the effect of NB presence on the micelle structure.

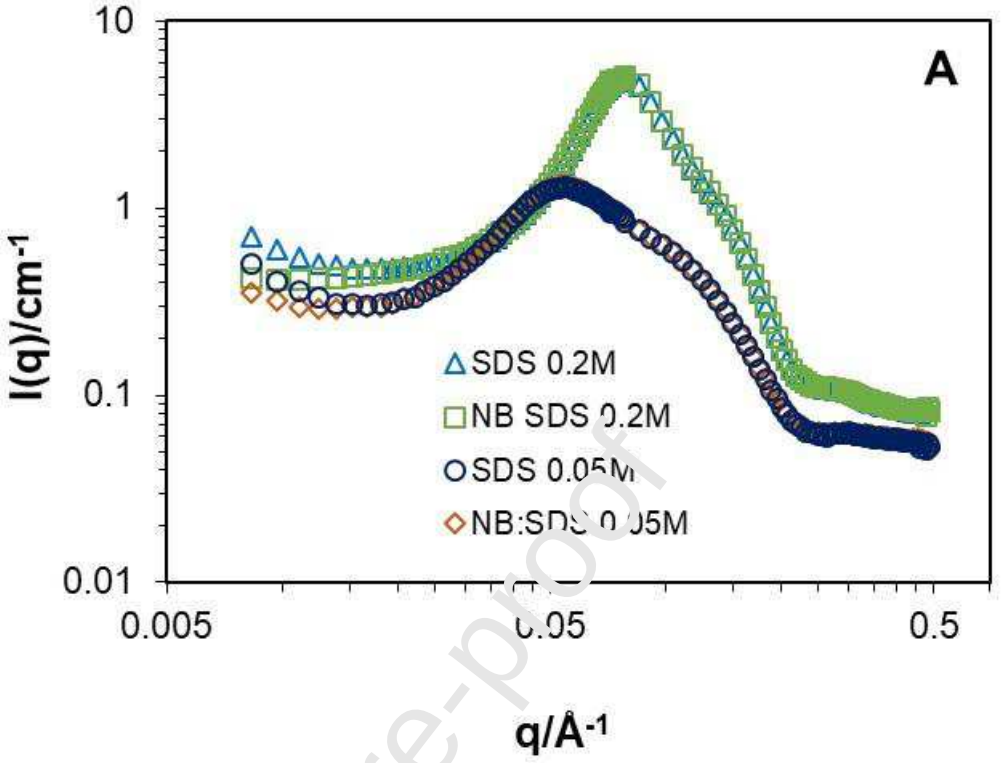

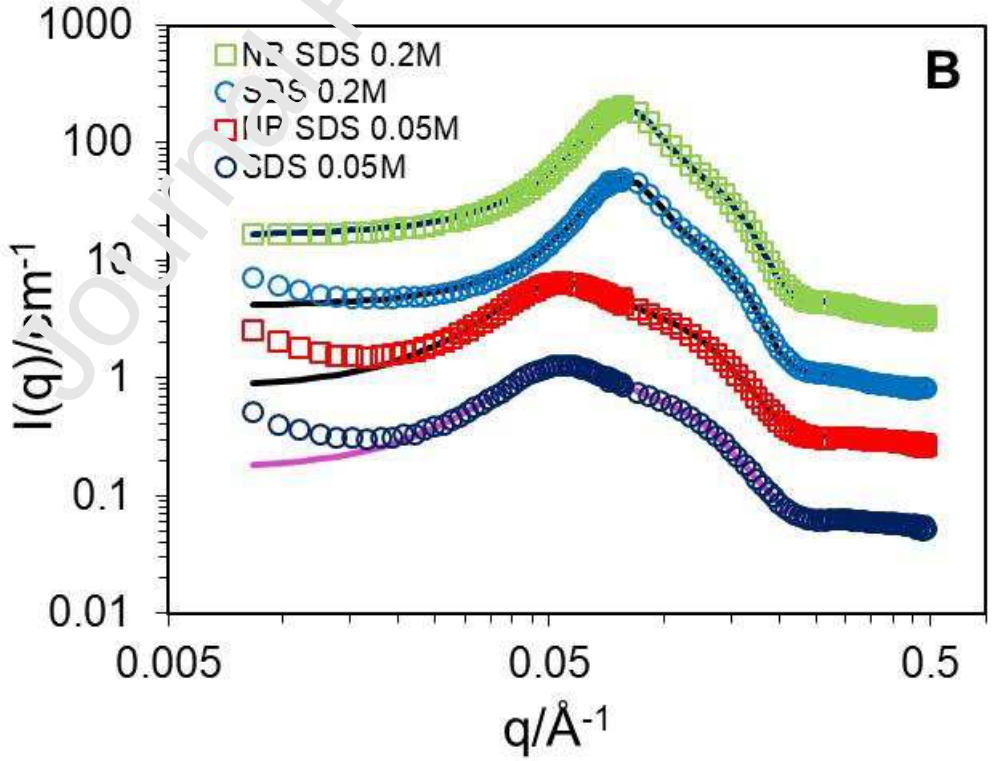

Figure 3: Small-angle neutron scattering data of SDS micelles free (circles and triangles) and loaded with 1 mM NB (squares and diamonds), at 0.05 M (○,◊) and 0.2 M (Δ, □) of SDS concentration, in D_2O at 25 ºC. **A:** free and loaded micelles curves at both SDS concentrations. **B:** the same curves as in A, but staggered for better visibility. The fits (solid lines) correspond to the ellipsoidal micelle model [23,24].

Ellipsoid	**Polar Radius/Å**	**Equatorial Radius/Å**	**Charge/e**	**Volume fraction**	**Nagg**
SDS	14.29 ± 0.039	22.31 ± 0.027	16.79 ± 0.068	0.0125	46
NB:SDS	14.26 ± 0.039	22.42 ± 0.027	17.70 ± 0.072	0.0119	47
SDS	15.04 ± 0.011	23.14 ± 0.011	53.61 ± 0.540	0.0484	55
NB:SDS	15.06 ± 0.014	23.19 ± 0.011	52.57 ± 0.492	0.0486	54

Table 1: Fitting parameters to ellipsoid model of SANS curves of the free and 1mM NB-loaded SDS *0.05M* (files 1 and 2) and *0.2M* (files 3 and 4) in D_2O, at 298 K.

It is clear that free and loaded micelle changes with SDS concentration, as showed by the fitting parameters, summarized in Table 1. The charge on the micelle surface significantly increases with SDS concentration probably due to the increase of micellar surface. SANS curves reflect the higher Coulomb repulsion between the electric double-layers of larger particles [52].

The increase in SDS concentration also promotes the micelles to grow up. As can be observed, micelle thickness increases, showing SDS monomers stretch in the aggregate, besides the aggregation number, which passes from 46 to 55, at 0.05 and 0.2M SDS concentration, respectively; these values are consistent with the mean value Nagg =50 ± 4 [53], reported for free SDS at different surfactant concentrations. These changes show that at 0.2M of SDS, micelle affords a more compact environment to NB, than at 0.05M, as suggested previously using pyrene as probe [41]. This change in the micelle compactness is likely to modify the spatial orientation of the NB lateral side chain relative to the naphthalene ring, what on the basis of the quenching of fluorescence observed at high surfactant concentration, promotes their interaction.

3.2. Photodegradation of Nabumetone in SDS

The photodegradation of NB was controlled by fluorescence at low and high drug concentrations (0.04 and 1 mM, respectively) in water and aqueous SDS solution (0.2M). The irradiation of NB results in a decrease of the NB emission band at λ_{max}=355 nm and in simultaneous appearance of a new band at λ_{max}=440 nm (S8), as previously observed in other media [12,18]. At low drug concentration, the plot of the fluorescence intensity at the maximum of both bands (F_{355} and F_{440}, respectively) vs. time shows a delay time in water (t_{dl}=4 min) (Figure 4A), not previously detected, and in SDS (t_{dl}=2 min) (Figure 4B), whereas small or practically no latency time was detected at large NB concentration (Figure 4C).

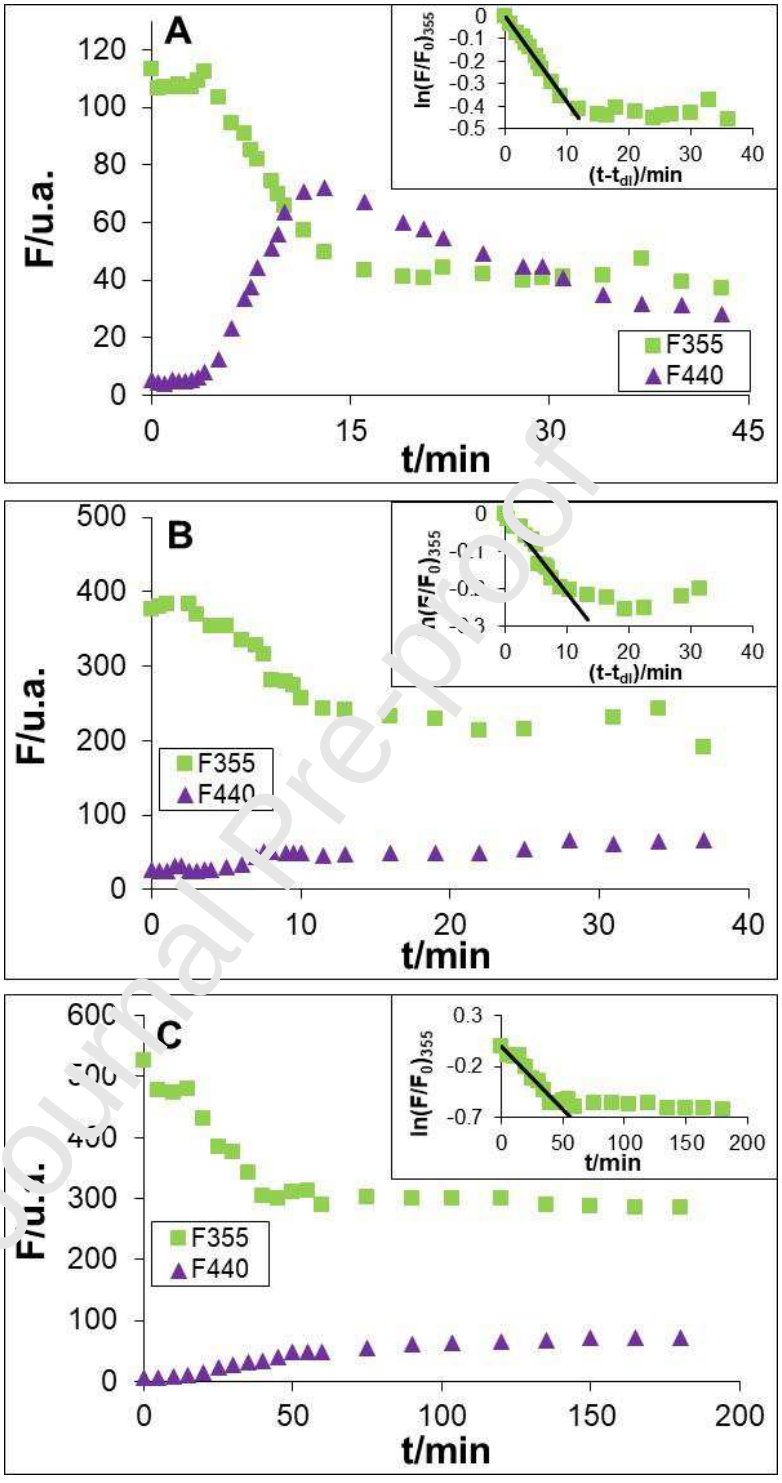

Figure 4: The plots of fluorescence intensity at 355 and 440 nm vs. irradiation time. **A:** 0.04 mM NB in water, **B:** 0.04 mM NB in 0.2M SDS, **C:** 1 mM NB in 0.2M SDS. *Insets* show the approximation by exponential function.

At large irradiation times, F_{440} in water decreases, (Figure 4A), showing that further transformation processes take place.

The photodegradation first order rate constants (k_{PD}) were obtained by fitting the decrease of F_{355} with irradiation time to the exponential function (Figure 4 inset) and quantum yields (ϕ_{PD}) (Table 2) were calculated as previously described [30].

System	$k_{PD}*10^4/s^{-1}$	ϕ_{PD}
NB_{dil}:H_2O	5.82 ± 1.35	$(2.03\pm0.5)*10^{-2}$
NB_{dil}:SDS	4.36 ± 0.88	$(1.52\pm 0.3)*10^{-2}$
NB_{conc}:SDS	3.10 ± 0.88	$(1.08\pm 0.3)*10^{-2}$

Table 2: The first order rate constants (k_{PD}) and quantum yield (ϕ_{PD}) of NB (dil – 0.04 mM and conc – 1 mM) photodegradation in H_2O and in 0.2M of SDS.

The photodegradation quantum yield, ϕ_{PD}, in water obtained in the present work, is lower than that previously reported [10]. In the latter, the contribution of fluorescence of the alcoholic photoproduct to F_{355} was subtracted by deconvolution of the spectral contour. In the present work, the contribution of this photoproduct could justify the observed difference.

In SDS, at both NB concentrations, ϕ_{PD} is significantly smaller than in water (Table 2). The inclusion of NB into the micelle results in the protection of NB from photodegradation.

This result somehow seems to be unexpected, since ϕ_{PD} increases in butanol, environment with lower polarity than water [10]. The protective effect of SDS can be associated with NB screening in a micelle due to the "super cage effect", as it was supposed for the antibiotic norfloxacin in SDS [15].

The fluorescence excitation spectra of the solution of 1mM NB in aqueous 0.2M of SDS at different times of photolysis are presented in Figure 5.

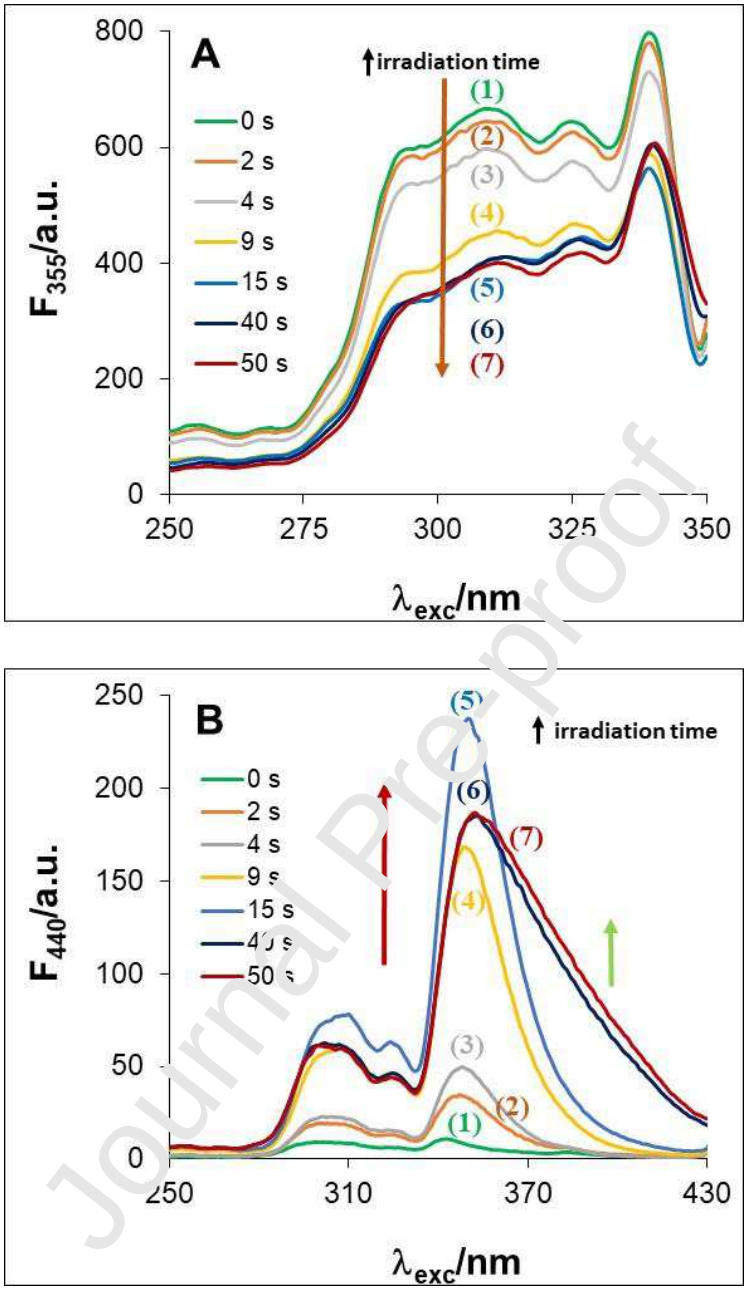

Figure 5: The fluorescence excitation spectra of irradiated samples of NB 1 mM in 0.2M SDS at different irradiation times: 0 (1), 2 (2), 4 (3), 9 (4), 15 (4), 40 (6), 50 (7) seconds. **A:** at the emission maximum of NB at λ_{em}=355 nm. **B:** at the emission maximum of the photoproducts at λ_{em}=440 nm.

The fluorescence excitation spectrum of irradiated samples at λ_{em}=355 nm (Figure 5A) shows NB degradation, and that at λ_{em}=440 nm (Figure 5B) demonstrates the appearance of at least

two photoproducts. The excitation spectrum at λ_{em}=440 nm presents two excitation maxima at λ_{exc}=310 and 350 nm. The band at λ_{exc}=310 nm was previously detected in water [9] and in butanol [10]. However, the band at λ_{exc}=350 nm was not observed. This band suggests the formation of one other photoproduct in SDS solution. The increase of the excitation intensity at $\lambda_{exc} \geq 370$ nm and decrease of that at $\lambda_{exc} \leq 370$ nm at large irradiation times assume that this photoproduct, at least in part, transforms into the next one.

3.2.1. High Performance Liquid Chromatography/Masses Spectrometry (HPLC/MS) study of NB Photoproducts

Next the structures of the photoproducts formed by 1mM NB in 0.2M SDS aqueous solution after 1h of irradiation were determined by means of HPLC/MS.

The chromatogram of the sample (S9, A) shows the most intense peaks with retention times of 18.8 min corresponding to the undegraded NB, and a second one at 17.9 min corresponding to the photoproduct formed. The mass spectrum of non-degraded NB was previously reported [9]. Mass spectrum of the peak appearing at shorter retention time (S9, B) with an intense peak with M: 213, was assigned to 2- (but-2-en-1-yl)-6-methoxynaphthalene **(2)** (Scheme 1), correspond to the photoproduct formed after NB irradiation in SDS. Although one photoproduct was just found, excitation spectra (see previous section) suggested the formation of two photoproducts one from the other. So, it is possible to speculate that this photoproduct found in SDS is a secondary one formed from the alcohol dehydration of the compound 4-(6-methoxy-2-naphtyl)-2-butanol, **(3)** (Scheme 2, *left*). This photoproduct was not found in any media where the NB photodegradation was studied [9][10][54][55]. It is worthy to know that 6-methoxy- 2-naphthaldehyde **(4)** (Scheme 2, *center*) was the major photoproduct found in water [9] and in n-butanol [10]. This later compound could also be formed after further oxidation of the lateral side chain from **(2)** detected in SDS (Scheme 1).

The results all together suggest NB degradation happens by a stepwise processes involving the initial carbonyl photoreduction and further oxidations of the lateral side chain.

Interestingly, NB metabolism in liver occurs by two mechanisms: ketone reduction and oxidative cleavage of the lateral side chain. NB hepatic reduction, yields **(3)**, (Scheme 2 *left*) by a not well known, but highly stereospecific mechanism. Whereas, by oxidation NB yields 6-methoxy-2-naphtyl acetic acid **(5)** (Scheme 2, right) with the lateral side chain oxidized up to the acidic compound which is the active metabolite of the NB [56].

(3)

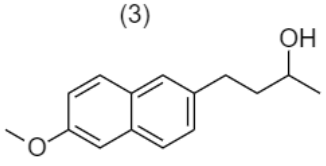

4-(6-methoxy-2-naphtyl)-2-butanol

(4)

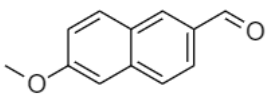

6-methoxy-2-naphthaldehyde

(5)

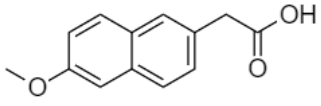

6-methoxy-2-naphtyl acetic acid

Scheme 2: Chemical structure of: **(3)** probable primary photoproduct formed in SDS which has

the same structure than the metabolite formed by metabolic reduction of the NB (*left*); **(4)** main photoproduct found in homogeneous media by NB irradiation (*center*); and **(5)** NB metabolite formed in the liver by drug oxidation in liver (*right*).

Therefore the loading of the NB in the SDS micelle protects the drug to the oxidative reactions of the lateral side chain.

And the reactivity of the drug in SDS against light seems to be closely related to the biological enzymatic degradation of the NB after oral administration.

3.2.2. Intermediates of photolysis of NB in aqueous micellar solutions of SDS

The nanosecond laser flash photoexcitation of NB in aqueous SDS solution results in the formation of three intermediates characterized by transient absorption with maxima at 440, 630 and 720 nm observed immediately after the laser pulse and by significantly different lifetimes (30 μs, 1000 μs and 1μs, respectively) (Figure 6, curve A).

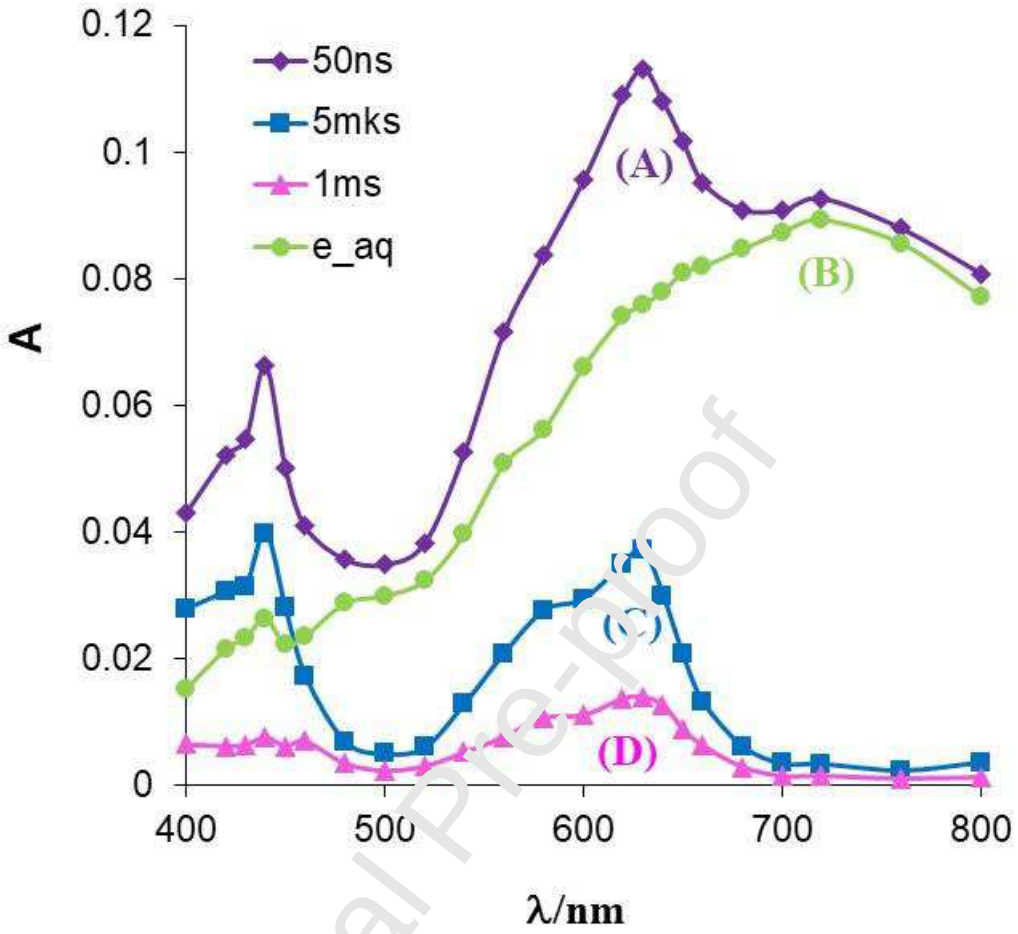

Figure 6: UV-vis transient absorption spectra of intermediates obtained upon laser flash photolysis of deaerated aqueous solutions of NB (1 mM) in the presence of SDS (0.2 M) at 0.05 (A), 5 (C) and 1000 (D) μs after the laser pulse (337 nm) and (B) is the difference of absorption spectra (A) and (C) representing the absorption spectra of e_{aq}^{SDS}.

The relatively narrow band with maximum at 440 nm is the characteristic of NB triplet excited state (^{3}NB) and that at 630 nm is the absorption of NB radical cation ($NB^{+\bullet}$), as it was previously described in homogeneous solutions [4]. The short lived relatively broad absorption with the well known characteristic maximum around 720 nm can be assigned to the hydrated electron e_{aq}^{SDS} [57].

The e_{aq}^{SDS} absorption spectra calculated by subtraction of the initial transient absorption and the residual transient absorption observed after e_{aq}^{SDS} decay (Figure 6, curve B) practically coincides with that in pure water showing that e_{aq}^{SDS} is localized in a water phase.

The quadratic dependence of e_{aq}^{SDS} and $NB^{+\bullet}$ yields on laser energy is observed as already reported for the photogeneration of $NB^{+\bullet}$ in different polar homogeneous solutions [4].

Therefore, a biphotonic process is responsible for the formation of e_{aq}^{SDS} and $NB^{+\bullet}$. The photoionization of NB in SDS solution observed under the present experimental conditions seems to be rather efficient demonstrating the effective charge separation effect instead of backward recombination of e_{aq}^{SDS} and $NB^{+\bullet}$. One can suppose that NB is localized in the vicinity of the micellar surface where the negative charge of SDS heads facilitates the charge separation.

The e_{aq}^{SDS} decay kinetics in deaerated solutions obeys a monoexponential law with first order rate constant (k_e) near $1*10^6$ s^{-1}. On one hand this value seems to be an order of magnitude larger than the expected one for the hydrated electron in pure water ($\leq 1*10^5$ s^{-1} [57]).

On the other hand the characteristic rate constant of the diffusion controlled recombination of the pair of particles in SDS micelle is of the order of $1\bullet10^7$ s^{-1} [58–61]. However, e_{aq}^{SDS} decay is significantly longer. Moreover, the lifetime of $NB^{+\bullet}$ is significantly longer than that of e_{aq}^{SDS} (see below). Therefore e_{aq}^{SDS} escapes from the micelle to the water bulk due to the electrostatic repulsion from the negatively charged micelle.

Solvated electron was not observed in the course of NB photoionization in homogeneous polar solvents and even in water (with 20% of acetonitrile) [4]. It was supposed that the solvated electron is short-lived in homogeneous solution because of the ketone moiety of NB acting as an electron scavenger. The corresponding aliphatic ketone radical anion would be transparent at the wavelengths monitored. However, the decay of e_{aq}^{SDS} accelerates only insignificantly with [NB] increase. The value of k_e increases from $0.71*10^6$ s^{-1} to $1.1*10^6$ s^{-1} with [NB] increase from 0.5 to 3 mM. The slight dependence of k_e on [NB], shows that NB localized in micellar phase, is screened from e_{aq}^{SDS} in the water phase. Therefore, one can assume that e_{aq}^{SDS} is quenched by the residual amount of NB in the water phase which is near 0.4 mM. In this case, the close to diffusion-controlled quenching of e_{aq}^{SDS} by NB occurs with rate constant of the order of $2*10^9$ $M^{-1}s^{-1}$ which agrees with the lack of solvated electron observation in microsecond time scale in relatively concentrated homogeneous NB solutions

The quenching of e_{aq}^{SDS} by molecular oxygen is controlled by diffusion. The value of corresponding rate constant equal to $k = 1.6*10^{10}$ $M^{-1}s^{-1}$ was estimated using the oxygen concentration of 0.28 mM in air saturated water. The formation of reactive radical $O_2^{-\bullet}$ is expected.

The ^3NB and $NB^{+\bullet}$ absorption is observed after e_{aq}^{SDS} decay was complete (Figure 6, curve C).

The ^3NB decay kinetics in deaerated SDS solution is monoexponential with first order rate constant $3.1*10^4$ s^{-1}, which is significantly smaller than that measured for e_{aq}^{SDS}. This value is very similar to those reported for ^3NB decay in homogeneous media [4], where it was assumed that the presence of the butanone substituent controls the decay of NB excited states due to β-aryl quenching [4]. In contrast to the homogeneous media, the self quenching of ^3NB was not observed in SDS solution because of small diffusion coefficient of ^3NB localized in micellar phase.

Triplet state of many ketones is able to abstract hydrogen from suitable substrates [62]. Simple aliphatic hydrocarbons are able to provide protons for the ketone photoreduction [63]. This primary process results finally in the carbonyl group reduction [62,64].

It was discussed already and confirmed experimentally that ^{3}NB is not such reactive as ketone triplet states toward hydrogen abstraction even from strong hydrogen donors [4]. However, one can suppose that there is some side process of ^{3}NB decay which is the reduction of the carbonyl group with formation of the corresponding alcohol derivative.

The quenching of ^{3}NB by molecular oxygen, is controlled by diffusion with spin-statistical factor 1/9, which is the characteristic of triplet-triplet energy transfer. The value of corresponding rate constant equal to $1.5*10^9$ $M^{-1}s^{-1}$ was calculated using the oxygen concentration in air saturated water 0.28 mM. The formation of reactive singlet oxygen $^1O_2$ is expected as it was observed in homogeneous media [5].

The transient absorption of $NB^{+\bullet}$ remained even after the decay of the ^{3}NB was complete and besides the most important band at 430 nm, it showed additional bands near 450 nm described for $NB^{+\bullet}$ and other naphthalene-like radical cations (Figure 6, curve D) [3,4][65].

The lifetime of $NB^{+\bullet}$ in SDS solution under the experimental condition was $\geq$ 0.5 ms and increased with the decrease of initial $NB^{+\bullet}$ concentration. This lifetime is an order of magnitude longer than that observed for $NB^{+\bullet}$ in polar organic solvents and even in water with 20% of acetonitrile [4]. The first order decay kinetics of $NB^{+\bullet}$ independent on the NB concentration was observed in homogeneous media and it was assigned to some reaction in the presence of butanone side-chain. The decay kinetics of $NB^{+\bullet}$ in SDS solution was independent on [NB]. Thus, a dimer formation between NB radical cation and NB is not important under the experimental conditions used in the present work. This observation is in contrast to that for radical cations of naphthalene and some derivatives which reacts with their ground state to form radical cation of dimer at large enough concentration of naphthalene [65][66].

In spite of the fact that electron donating substituents in naphthalene moiety favors the dimer cation formation, in the case of NB in SDS solution, the micelle prevents the bimolecular reaction of $NB^{+\bullet}$ in one micelle with NB in the other. Although the minor amounts of dimers can be formed in reaction of $NB^{+\bullet}$ with residual NB in water phase or in small number of micelles with the couple of NB.

Surprisingly, the decay kinetics of $NB^{+\bullet}$ in SDS solution followed the second order kinetics and it was independent on the presence of air. The corresponding values of $k_2/\varepsilon l$, were k_2 is the second order rate constant, ε is $NB^{+\bullet}$ extinction coefficient and l is the optical path length, were obtained by fitting the experimental decay kinetics. In order to extract the extinction coefficient, the absorption of $NB^{+\bullet}$ was compared with that of e_{aq}^{SDS} (see Fig. 6, spectra B and C). It is reasonable to suppose that e_{aq}^{SDS} and $NB^{+\bullet}$ are formed in equal amount. The value $\varepsilon = 7.4*10^3$ $M^{-1}cm^{-1}$ at 630 nm was obtained using e_{aq}^{SDS} extinction coefficient equal to that in water ($1.85*10^4$ $M^{-1}cm^{-1}$ [57]). Then the calculated value is $k_2 = 8.9*10^8$ $M^{-1}s^{-1}$ which is somewhat smaller than the diffusion-controlled one, suggesting that $NB^{+\bullet}$ is protected in the negatively charged micelle. So, it can be assumed that $NB^{+\bullet}$ localized in SDS micelle reacts with negatively charged NB derivative which appeared in reaction of e_{aq}^{SDS} or $O_2^{-\bullet}$ with residual NB in the water phase (see above).

Therefore, the behavior of transient photoproducts of NB in aqueous SDS solution differs significantly from that in homogeneous environment. On one hand, the formation of active form of oxygen is still efficient and thus NB could be a potential photosensitizer contributing

to the overall phototoxicity. On the other hand, the radical cation of NB is isolated in micellar phase and the most important pathway of its decay seems to be the regeneration of NB with probable minor formation of some dimer-like forms.

4. Conclusion

The results obtained in the present work show the significant difference in photochemical behavior of NB in aqueous SDS micellar solution with respect to that in homogeneous liquids. The fluorescence study demonstrates that NB is localized in micellar phase. The most important difference seems to be the protection of NB in SDS micelles from photodegradation due to a slow down or perhaps a change in the reactions involved in its mechanism. The quantum yield of photodegradation is smaller in micellar system than that in homogeneous solvents including water. Moreover, a different final photoproduct, 2- (but-2-en-1-yl)-6-methoxynaphthalene, is formed. This photoproduct formation shows that the probability of NB lateral side chain oxidation is decreased in SDS compared to homogeneous media. The formation and decay of NB transients studied by the laser flash photolysis revealed the principal differences from those in homogeneous solutions. The primary events after photoexcitation of NB in SDS micellar solution demonstrate the regeneration of NB due to its isolation and protection in micellar phase as the most important pathway. The photoproduct seems to be formed from the ^{3}NB by hydrogen substraction from the SDS hydrocarbon chains. The comparative study of the drug behavior in homogeneous and organized environment may have some applications after additional studies in different systems.

Acknowledgement

This work is based upon experiments performed at the KWS-2 instrument operated by JCNS at the Heinz Maier-Leibnitz Zentrum (MLZ), Garching, Germany.

References

[1] S.H. Roth, Nabumetone: Therapeutic use and safety profile in the management of osteoarthritis and rheumatoid arthritis: Commentary, Drugs. 64 (2004) 2344–2345. https://doi.org/10.2165/00003495-200464200-00005.

[2] S.A. Khan, M.K. McLean, Toxicology of Frequently Encountered Nonsteroidal Anti-Inflammatory Drugs in Dogs and Cats, Vet. Clin. North Am. - Small Anim. Pract. 42 (2012) 289–306. https://doi.org/10.1016/j.cvsm.2012.01.003.

[3] F. Boscá, M.L. Marín, M.A. Miranda, Photoreactivity of the Nonsteroidal Anti-inflammatory 2-Arylpropionic Acids with Photosensitizing Side Effects¶, Photochem. Photobiol. 74 (2001) 637–651. https://doi.org/10.1562/0031-8655(2001)074<0637:potnai>2.0.co;2.

[4] L.J. Martínez, J.C. Scaiano, Characterization of the Transient Intermediates Generated from the Photoexcitation of Nabumetone: A Comparison with Naproxen, in: Photochem. Photobiol., 1998: pp. 646–651. https://doi.org/10.1111/j.1751-1097.1998.tb02524.x.

[5] A.S. N. Canudas, J. Moulinier, D. Zamora, Photobiological properties of nabumetone (4-[6-methoxy-2-naphthalenyl]-2-butanone), a novel non-steroidal anti-inflammatory and analgesic agent, Pharmazie. 55 (2000) 282–285.

[6] M. Mezzelani, S. Gorbi, F. Regoli, Pharmaceuticals in the aquatic environments: Evidence of emerged threat and future challenges for marine organisms, Mar. Environ. Res. 140 (2018) 41–60. https://doi.org/10.1016/j.marenvres.2018.05.001.

[7] Q. Peng, J. Song, X. Li, H. Yuan, N. Li, L. Duan, Q. Zhang, X. Liang, Biogeochemical characteristics and ecological risk assessment of pharmaceutically active compounds (PhACs) in the surface seawaters of Jiaozhou Bay, North China, Environ. Pollut. 255 (2019) 113247. https://doi.org/10.1016/j.envpol.2019.113247.

[8] A.J. Ebele, M. Abou-Elwafa Abdallah, S. Harrad, Pharmaceuticals and personal care products (PPCPs) in the freshwater aquatic environment, Emerg. Contam. 3 (2017) 1–16. https://doi.org/10.1016/j.emcon.2016.12.004.

[9] M. Valero, S.M.B. Costa, Photodegradation of Nabumetone in aqueous solutions, J. Photochem. Photobiol. A Chem. 157 (2003) 93–101. https://doi.org/10.1016/S1010-6030(03)00013-3.

[10] M. Valero, Photodegradation of Nabumetone in n-butanol solutions, J. Photochem. Photobiol. A Chem. 163 (2004) 159–164. https://doi.org/10.1016/j.jphotochem.2003.11.005.

[11] S. Sortino, L.J. Martínez, G. Marconi, On the photophysical and photochemical behavior of fenbufen: A study in homogeneous media and micellar environments, New J. Chem. 25 (2001) 975–980. https://doi.org/10.1039/b100164g.

[12] P. Opanasopit, T. Ngawhirunpat, T. Rojanarata, C. Choochottiros, S. Chirachanchai, N-Phthaloylchitosan-g-mPEG design for all-trans retinoic acid-loaded polymeric micelles, Eur. J. Pharm. Sci. 30 (2007) 424–431. https://doi.org/10.1016/j.ejps.2007.01.002.

[13] C. Lu, X. Yin, X. Liu, M. Wang, Study of the photodegradation kinetics and pathways of Hexaflumuron in liquid media, Photochem. Photobiol. 90 (2014) 1219–1223. https://doi.org/10.1111/php.12314.

[14] K. Huang, G. Lu, Z. Zheng, R. Wang, T. Tang, X. Tao, R. Cai, Z. Dang, P. Wu, H. Yin, Photodegradation of 2,4,4′-tribrominated diphenyl ether in various surfactant solutions: Kinetics, mechanisms and intermediates, Environ. Sci. Process. Impacts. 20 (2018) 806–812. https://doi.org/10.1039/c8em00033f.

[15] S. Sortino, Selective Entrapment of the Cationic Form of Norfloxacin within Anionic Sodium Dodecyl Sulfate Micelles at Physiological pH and its Effect on the Drug Photodecomposition†, Photochem. Photobiol. 82 (2006) 64–70. https://doi.org/10.1562/2005-06-01-ra-560.

[16] S. Sortino, G. de Guidi, S. Guiffrida, Drastic photochemical stabilization of Lomefloxacin through selective and efficient self-incorporation of its cationic form in anionic sodium dodecyl sulfate (SDS) micelles, New J. Chem. 25 (2001) 197–199. https://doi.org/10.1039/b008257k.

[17] D.S. Pellosi, B.M. Estevão, J. Semensato, D. Severino, M.S. Baptista, M.J. Politi, N. Hioka, W. Caetano, Photophysical properties and interactions of xanthene dyes in aqueous micelles, J. Photochem. Photobiol. A Chem. 247 (2012) 8–15. https://doi.org/10.1016/j.jphotochem.2012.07.009.

[18] M. Valero, L.J. Rodriguez, M.M. Velazquez, Inclusion of non-steroidal anti-inflammatory agents into aqueous cyclodextrins: A UV-absorption spectroscopic study, Farmaco. 51 (1996) 525–533.

[19] G.T. Rich, R.M. Faulks, M.S.J. Wickham, A. Fillery-Travis, Solubilization of carotenoids from carrot juice and spinach in lipid phases: II. Modeling the duodenal environment, Lipids. 38 (2003) 947–956. https://doi.org/10.1007/s11745-003-1148-z.

[20] M. Buchweitz, P.A. Kroon, G.T. Rich, P.J. Wilde, Quercetin solubilisation in bile salts: A comparison with sodium dodecyl sulphate, Food Chem. 211 (2016) 356–364. https://doi.org/10.1016/j.foodchem.2016.05.024.

[21] A.N. Fletcher, Quinine sulfate as a fluorescence quantum yield standard, Photochem. Photobiol. (1969) 221–224. https://doi.org/10.1111/j.1751-1097.1969.tb07311.x.

[22] A. Radulescu, N.K. Szekely, M.S. Appavou, V. Pipich, T. Kohnke, V. Ossovyi, S. Staringer, G.J. Schneider, M. Amann, B. Zhang-Haagen, G. Brandl, M. Drochner, R. Engels, R. Hanslik, G. Kemmerling, Studying soft-matter and biological systems over a wide length-scale from nanometer and micrometer sizes at the small-angle neutron diffractometer KWS-2, J. Vis. Exp. 2016 (2016) 1–23. https://doi.org/10.3791/54639.

[23] L.A. Feigin, D.I. Svergun, Structure Analysis by Small-Angle X-Ray and Neutron Scattering, Plenum Press, new York, 1987.

[24] A. Isihara, Photoinduced phase separation in the lead halides is a polaronic effect, J. Chem. Phys. 13 (1950) 1446–1449.

[25] C.G. Malmberg, Dielectric constant of deuterium oxide, J. Res. Natl. Bur. Stand. (1934). 60 (1958) 609–612. https://doi.org/10.6028/jres.060.060.

[26] I. Grillo, I. Morfin, S. Prévost, Structural Characterization of Pluronic Micelles Swollen with Perfume Molecules, Langmuir. 34 (2018) 13395–13408. https://doi.org/10.1021/acs.langmuir.8b03050.

[27] H.H. Tönnensen, Photostability of Drugs and Drug Formulations, Second Edition, CRC Press, Boca Raton, 2004. https://doi.org/10.1201/9781420023596.

[28] H. Heath, A new sensitive chemical actinometer - II. Potassium ferrioxalate as a standard chemical actinometer, Proc. R. Soc. London. Ser. A. Math. Phys. Sci. 235 (1956) 518–536. https://doi.org/10.1098/rspa.1956.0102.

[29] G.W. Castellan, Physical Chemistry, 2nd ed., Addison Wesley S.A, México, 1987.

[30] T. Mill, W.R. Mabey, B.Y. Lan, A. Baraze, Photolysis of polycyclic aromatic hydrocarbons in water, Chemosphere. 10 (1981) 1281–1290. https://doi.org/10.1016/0045-6535(81)90045-X.

[31] P.P. Levin, N.B. Sul'timova, O.N. Chaikovskaya, Kinetics of fast reactions of triplet states and radicals under photolysis of 4,4′-dimethylbenzophenone in the presence of 4-halophenols in micellar solutions of sodium dodecyl sulfate in magnetic field, Russ. Chem. Bull. 54 (2005) 1433–1438. https://doi.org/10.1007/s11172-005-0423-0.

[32] N.B. Sul'timova, P.P. Levin, O.N. Chaikovskaya, Laser photolysis study of the transient products of 4-carboxybenzophenone-sensitized photolysis of chlorophenoxyacetic acid-based herbicides in aqueous micellar solutions, High Energy Chem. 44 (2010) 393–398. https://doi.org/10.1134/S0018143910050073.

[33] Y. Moroi, K. Motomura, R. Matuura, The critical micelle concentration of sodium dodecyl sulfate-bivalent metal dodecyl sulfate mixtures in aqueous solutions, J. Colloid Interface Sci. 46 (1974) 111–117. https://doi.org/10.1016/0021-9797(74)90030-7.

[34] J.H. Fendler, E.J. Fendler, Catalysis in micelar and macromolecular syntesis, Academic Press, 1975.

[35] B.L. Bales, A definition of the degree of ionization of a micelle based on its aggregation number, J. Phys. Chem. B. 105 (2001) 6798–6804. https://doi.org/10.1021/jp004576m.

[36] J.H. Collett, R. Withington, Partition coefficients of salicylic acid between water and the micelles of some non- ionic surfactants, J. Pharm. Pharmacol. 24 (1972) 211–214. https://doi.org/10.1111/j.2042-7158.1972.tb08966.x.

[37] P.D. Bryson, Nonsteroidal anti-inflammatory agents. In: Comprehensive review in toxicology for emergency clinicians, 3rd ed., Washington, DC, 1996.

[38] N. Devanna, M.R. Devi, Application of Spherical Agglomeration Technique To Improve Micromeritic Properties and Dissolution Characteristics of Nabumetone, Int. Res. J. Pharm. 3 (2012) 156–162.

[39] P.B. Rathi, K. V Deshpande, P.S. Panzade, J. Roul, Nabumetone solubility prediction in dioxane-water mixtures using extended Hildebrand solubility approach., Asian J. Biomed. Pharm. Sci. 3 (2013) 33–37. http://jbiopharm.com/index.php/ajbps/article/view/.

[40] M. Valero, S.M.B. Costa, J.R. Ascenso, M.M. Velázquez, L.J. Rodríguez, Complexation of the non-steroidal anti-inflammatory drug Nabumetone with modified and unmodified cyclodextrins, J. Incl. Phenom. 35 (1999) 663–677. https://doi.org/10.1023/A:1008011228459.

[41] W. Liu, R. Guo, Interaction between morin and sodium dodecyl sulfate (SDS) micelles, J. Agric. Food Chem. 53 (2005) 2890–2896. https://doi.org/10.1021/jf047847p.

[42] A. Chahti, M. Boukalouch, J.P. Dumas, A. El Kinani, Phase transitions in colloidal systems. Part I. Refractometric study of the binary system SDS+water or pentanol-1+water and the ternary system water+SDS+pentanol-1 at 298.15 K, J. Dispers. Sci. Technol. 21 (2000) 525–535. https://doi.org/10.1080/01932690008913288.

[43] M. Valero, S.M.B. Costa, M.A. Santos, Conformations of a non-steroidal anti-inflammatory drug nabumetone in aqueous environments, J. Photochem. Photobiol. A Chem. 132 (2000) 67–74. https://doi.org/10.1016/S1010-6030(99)00253-1.

[44] I. Novak, B. Kovač, On the biological activity of drug molecules: Busulfan and nabumetone, Chem. Phys. Lett. 498 (2010) 240–244. https://doi.org/https://doi.org/10.1016/j.cplett.2010.08.073.

[45] V.K. Aswal, P.S. Goyal, Counterions in the growth of ionic micelles in aqueous electrolyte solutions: A small-angle neutron scattering study, Phys. Rev. E - Stat. Physics, Plasmas, Fluids, Relat. Interdiscip. Top. 61 (2000) 2947–2953. https://doi.org/10.1103/PhysRevE.61.2947.

[46] P.A. Hassan, G. Fritz, E.W. Kaler, Small angle neutron scattering study of sodium dodecyl sulfate micellar growth driven by addition of a hydrotropic salt, J. Colloid Interface Sci. 257 (2003) 154–162. https://doi.org/10.1016/S0021-9797(02)00020-6.

[47] X. Ye, T. Narayanan, P. Tong, J.S. Huang, Neutron scattering study of depletion interactions in a colloid-polymer mixture, Phys. Rev. Lett. 76 (1996) 4640–4643. https://doi.org/10.1103/PhysRevLett.76.4640.

[48] K.H. Lin, J.C. Crocker, A.C. Zeri, A.G. Yodh, Colloidal interactions in suspensions of rods, Phys. Rev. Lett. 87 (2001) 88301-1–88301–4. https://doi.org/10.1103/PhysRevLett.87.088301.

[49] P.W. Schmidt, Collimation effects in small x-ray ad neutron scattering, J.Appl. Cryst. 21 (1988) 602–612.

[50] E.G.R. Putra, A. Patriati, Structural and phase transition changes of sodium dodecyl sulfate micellar solution in alcohols probed by small-angle neutron scattering (SANS), AIP Conf. Proc. 1656 (2015). https://doi.org/10.1063/1.4917088.

[51] J.B. Hayter, J. Penfold, Determination of micelle structure and charge by neutron small-angle scattering, Colloid Polym. Sci. 261 (1983) 1022–1030. https://doi.org/10.1007/BF01421709.

[52] J.B. Hayter, A rescaled MSA structure factor fordiluted charged colloidal dispersions, Mol. Phys. 46 (1982) 651–656.

[53] B.L. Bales, L. Messina, A. Vidal, M. Peric, O.R. Nascimento, Precision relative aggregation number determinations of SDS micelles using a spin probe. A model of micelle surface hydration, J. Phys. Chem. B. 102 (1998) 10347–10358. https://doi.org/10.1021/jp983364a.

[54] M.C. Jiménez, M.A. Miranda, R. Tormos, Photochemistry of naproxen in the presence of β-cyclodextrin, J. Photochem. Photobiol. A Chem. 104 (1997) 119–121. https://doi.org/10.1016/s1010-6030(97)00013-0.

[55] I.O.P.C. Series, M. Science, Cyclodextrins in topical gel formulation as photoprotective system for Cyclodextrins in topical gel formulation as photoprotective system for Nabumetone, (2020). https://doi.org/10.1088/1757-899X/777/1/012005.

[56] P. Malátková, V. Wsól, Carbonyl reduction pathways in drug metabolism, Drug Metab. Rev. 46 (2014) 96–123. https://doi.org/10.3109/03602532.2013.853078.

[57] M.A. Hart, The Hydrated Electron, John Wiley & Sons Original, 1970.

[58] A. Malliaris, J. Le Moigne, J. Sturm, R. Zana, Temperature dependence of the micelle aggregation number and rate of intramicellar excimer formation in aqueous surfactant solutions, J. Phys. Chem. 89 (1985) 2709–2713. https://doi.org/10.1021/j100258a054.

[59] N.J. Turro, M. Okamoto, P.L. Kuo, Pressure effects on the fluorescence decay of pyrene in micellar solutions, J. Phys. Chem. 91 (1987) 1819–1823. https://doi.org/10.1021/j100291a028.

[60] C. Bohne, D. Griller, J.C. Scaiano, M.S. Alnajjar, Example of Diffusion-Limited Behavior in the Reaction of a Geminate Radical Pair in Micelles, J. Am. Chem. Soc. 113 (1991) 1444–1445. https://doi.org/10.1021/ja00004a072.

[61] P.P. Levin, V.Y. Shafirovich, V.A. Kuzmin, Magnetic isotope effects on the decay kinetics of micellized triplet ketyl-phenoxyl radical pairs. Role of hyperfine, exchange, and dipole-dipole interactions, J. Phys. Chem. (1992). https://doi.org/10.1021/j100203a083.

[62] G.S. Hammond, N. Turro, Organic Photochemistry, Science (80-.). 142 (1963) 1541–1553.

[63] N.C. Yang, D.H. Yang, Photochemical reactions of ketones in solution, J. Am. Chem. Soc. 80 (1958) 2913–2914. https://doi.org/https://doi.org/10.1021/ja01544a092.

[64] G. Porter, P. Suppan, No Title, Proc. Chem. Soc. 191 (1964).

[65] S. Steenken, C.J. Warren, B.C. Gilbert, Generation of radical-cations from naphthalene and some derivatives, both by photoionization and reaction with so4-: Formation and reactions studied by laser flash photolysis, J. Chem. Soc. Perkin Trans. 2. (1990) 335–342. https://doi.org/10.1039/p29900000335.

[66] A.V.K. P.P Levin, Laser photolysis study of triplet exciplexes of chloranil with naphthalenes, Chem. Bull. Int. Ed. (Bull. Acad. Sci. USSR, Div. Chem. Sci.). 3 (1998) 515–519. https://doi.org/0568-5230/88/3703-0429512.50.

Figure Captions

Figure 1: Plot of the ratio of NB solubility in SDS and in water ($S_0^{SDS}/S_0^{H_2O}$|) vs. SDS volume fraction (ϕ_{SDS}). The line is the fitting to the linear function.

Figure 2. A: The plot of fluorescence intensity at 355 nm, F_{355}, of NB, 4×10^{-5}M (●) and: 1 mM (▲) (*Inset)* and **B** - Refractive index of all the samples, 0.04 and 1mM of NB vs. SDS concentration (●). Black solid line in A and B is the fitting to a logistic equation [19][20].

Figure 3: Small-angle neutron scattering data of SDS micelles free (circles and triangles) and loaded with 1 mM NB (squares and diamonds), at 0.05 M (○,▽) and 0.2 M (**Δ,** □) of SDS concentration, in D_2O at 25 ºC. **A:** free and loaded micelles curves at both SDS concentrations. **B:** the same curves as in A, but staggered for better visibility. The fits (solid lines) correspond to the ellipsoidal micelle model [23, 24].

Figure 4: The plots of fluorescence intensity at 355 and 440 nm vs. irradiation time. **A:** 0.04 mM NB in water, **B:** 0.04 mM NB in 0.2M SDS, **C:** 1 mM NB in 0.2M SDS. *Insets* show the approximation by exponential function.

Figure 5: The fluorescence excitation spectra of irradiated samples of NB 1 mM in 0.2M SDS at different irradiation times: 0 (1), 2 (2), 4 (3), 9 (4), 15 (4), 40 (6), 50 (7) seconds. **A:** at the emission maximum of NB at λ_{em}=355 nm. **B:** at the emission maximum of the photoproducts at λ_{em}=440 nm.

Figure 6: UV-vis transient absorption spectra of intermediates obtained upon laser flash photolysis of deaerated aqueous solutions of NB (1 mM) in the presence of SDS (0.2 M) at 0.05 (A), 5 (C) and 1000 (D) μs after the laser pulse (337 nm) and (B) is the difference of absorption spectra (A) and (C) representing the absorption spectra of e_{aq}^{SDS}.

Scheme 1: Chemical structure of nabumetone **(1)** (*left*) and the photoproduct found after drug irradiation in aqueous SDS solution **(2)** (*right*).

Scheme 2: Chemical structure of: **(3)** probable primary photoproduct formed in SDS which has the same structure than the metabolite formed by metabolic reduction of the NB (*left*); **(4)**

main photoproduct found in homogeneous media by NB irradiation (*center*); and **(5)** NB metabolite formed in the liver by drug oxidation in liver (*right*).

CRediT author statement

Margarita Valero: Conceptualization; Methodology; Formal Analysis; Investigation; Writing Original draft.

Peter P. Levin: Investigation. Writing Original draft.

Natalya B. Sultimova: Investigation

Judith E. Houston: Investigation. Writing –Review & Editing.

Declaration of interests

☒ The authors declare that they have no known competing financial interests or personal relationships that could have appeared to influence the work reported in this paper.

☐The authors declare the following financial interests/personal relationships which may be considered as potential competing interests:

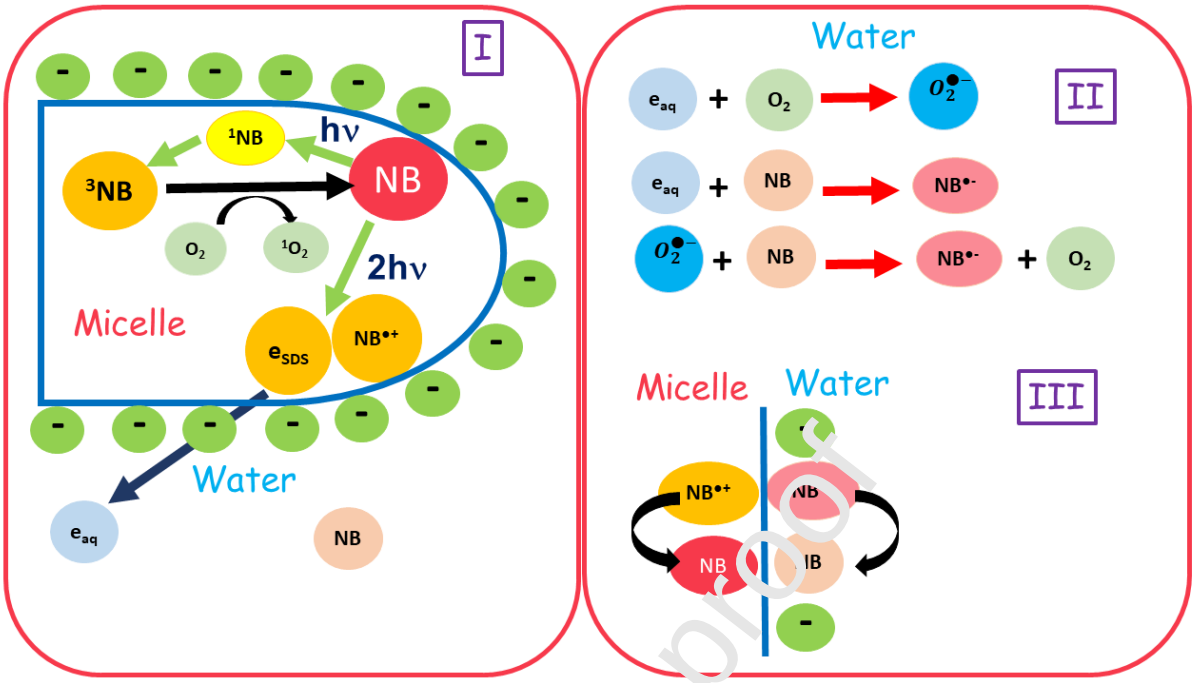

Graphical abstract

Highlights

Nabumetone strongly partitions inside the sodium dodecylsulfate micelles
Nabumetone fluorescence intensity is sensitive to the micellar structure
Aqueous sodium dodecylsulfate micelles protects nabumetone against photodegradation
Solvated electrons from NB are detected in the micellar environment
Triplet excited state is the precursor of the reduced nabumetone photoproduct